J. Fluid Mech. (1973), *vol.* 60, *part* 3, *pp.* 417–431
Printed in Great Britain

Dynamics of charge monolayers on insulating liquid interfaces

By J. R. MELCHER
Churchill College, Cambridge†

(Received 12 January 1973)

At most air–liquid interfaces stressed by a static perpendicular electric field, a monolayer of charge is induced that shields the field from the liquid. For relatively inviscid and highly insulating liquids, the electrohydrodynamics can dominate in determining the monolayer and field distributions associated with additional dynamic field components. Electric shear stresses lead to a convection of surface charge that distorts the field, much as though the liquid were conducting. A configuration for studying the monolayer dynamics is developed in which a uniform field is used to induce a uniform monolayer on the interface of a liquid layer having thickness c. Superimposed is a travelling wave of potential

$$\mathrm{Re}\,\hat{V}_0 \exp i(\omega t - kz),$$

imposed in a plane parallel to, and at a distance a above, the interface. Mechanisms for charge redistribution are reflected in the frequency response of the field transmitted through the interface to a second plane bounding the liquid layer from below. A model is developed which accounts for the self-consistent electromechanics in terms of the lumped surface parameters of surface charge σ_0 and surface mobility b_s and a bulk conductivity σ. According to this model, interfacial convection dominates at low frequencies in attenuating the field induced below the interface. For layers which are thick compared with the viscous skin depth, there is a resonance in the response at the frequency

$$\omega = \omega_i(2^{\frac{1}{3}}),$$

where

$$\omega_i = \{k\sigma_0^2/\epsilon_0(\rho\eta)^{\frac{1}{2}}\,[\coth ka + (\epsilon/\epsilon_0)\coth kc]\}^{\frac{2}{3}}$$

and ρ, η, ϵ_0 and ϵ are the liquid mass density, liquid viscosity, and permittivities of air and the liquid, respectively. Surface and bulk conduction, characterized by the relaxation time

$$\tau_b = \epsilon_0(\coth ka + (\epsilon/\epsilon_0)\coth kc)/[\sigma_0 b_s k + \sigma \coth kc],$$

result in a broadening of the resonance which is appreciable even for $\omega\tau_b \sim 5$. At frequencies high compared with both ω_i and $1/\tau_b$, the response is uninfluenced by the charge monolayer. Experiments substantiate the electroviscous resonance. A time-average surface force density, and associated steady convection of the

† Permanent address: Department of Electrical Engineering, Massachusetts Institute of Technology.

liquid, is also theoretically shown to be a consequence of the phase shifts caused by the electroviscous resonance. This is qualitatively demonstrated by measurement of the steady shear stress induced on the plane bounding the liquid from below.

1. Introduction

Charge monolayer in equilibrium

A monolayer of charge, shielding an electric field of intensity E_0 from the bulk of a liquid layer, is shown in figure 1. With a rudimentary model based on having particles of a single species, the thickness of the layer is pictured as determined by the balance between the tendency of charge to be brought to the interface by the electric field and the tendency for self-diffusion of the particles away from the region of high concentration at the interface. If the particles are described by a mobility b, related to the diffusion coefficient κ_D, Faraday constant F, gas constant R and temperature T by the Einstein relation $b = z\kappa_D F/RT$ (where z is the number of elementary charges carried by a particle), then the distribution of electric field intensity in the liquid is found to be

$$E_x = \frac{E_0(\epsilon_0/\epsilon)}{1 - x/l_D}, \quad l_D = 2RT/E_0(\epsilon_0/\epsilon)zF.$$

The 'thickness' l_D of this diffuse layer is approximated by taking $z = 1$ and $RT/F = 25{\cdot}6 \times 10^{-3}$ V (room temperature), and letting $E_0(\epsilon_0/\epsilon) = 10^6$ V/m, one-third of the breakdown strength of air, which gives $l_D \sim 5 \times 10^{-8}$ m.

With carriers of both signs contributing to the conduction, the charge monolayer structure can be pictured in terms of the Debye–Huckle theory commonly used to represent the diffuse part of a double layer (Delahay 1965). In that case the Debye length typifies the charge distribution. At extremely high surface charge densities, and certainly with films of a second phase on the interface, it is plausible that at least part of the charge can exist as a compact layer at the interface. That is, the charge particles may, in part, form a film capable of moving only within the interfacial plane.

Charge monolayer dynamics

The manner in which non-uniform dynamic fields redistribute the charge monolayer gives insight into the basic structure of the layer, and is of practical importance to the performance of liquid insulation subject to fields which have static components. Three mechanisms for redistribution of charge in the face of a non-uniform electric field are distinguished. In the first, the fluid reacts in a macroscopic mechanical sense to the shearing component of electric stress. The resulting charge convection is retarded by coupling through the viscous stress to the inertia of the liquid and to the surrounding boundaries. In the second, the tangential field results in charge conduction in the interfacial plane relative to the neutral liquid.

In the third, the dynamic electric field component normal to the charge layer in the liquid leads to charge redistribution through bulk conduction phenomena.

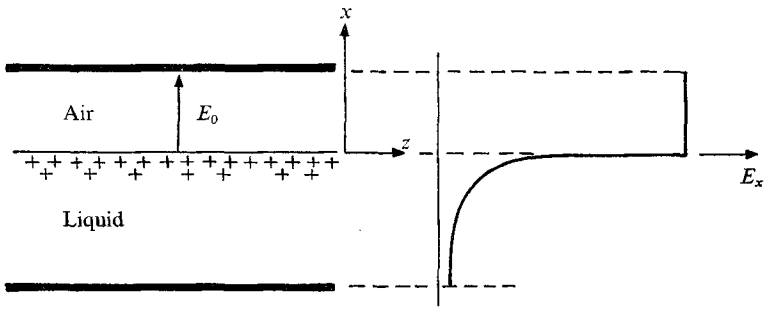

FIGURE 1. Charge monolayer in equilibrium. The thickness of a diffuse layer is determined by a balance between the upward electric force and self-diffusion from interfacial region of high concentration.

This is the dominant mechanism in semi-insulating, as opposed to highly insulating, materials.

Configuration

Under practical conditions, it is possible for all three mechanisms to play a role in determining the distribution of fields in the neighbourhood of a charged interface. To distinguish between the basic physical processes, it is necessary to have temporal and spatial control of both the fields and the associated flows. To this end, the configuration of figure 2 is used to subject the interface to a travelling wave of potential, and hence interfacial tangential electric field, having a predetermined frequency ω and wavenumber k. The linear electromechanical response then has the same wavenumber and frequency. Spatial periodicity is ensured by making the system re-entrant in an integral number of wavelengths.

Two types of measurements illustrate how the configuration can be used to examine the interaction mechanisms without introducing probes into the flow for purposes of making electrical and mechanical measurements. In the first of these, the linear response is measured by means of electrodes embedded in the earthed bottom plane. These electrodes are terminated in a sufficiently low resistance that they remain essentially at the same potential as the remainder of the plane. The frequency response of the current to these electrodes is partly determined by the response of the monolayer to the tangential electric field intensity. As will be developed in § 2, the response is characterized by an electroviscous resonance reflecting the redistribution of charge in the face of electric self-fields that stiffen the interface and inertial retardation from the liquid bulk viscously coupled to the interface.

A second type of response is nonlinear. Because of the phase shifts in the interfacial distribution of charge relative to the travelling wave of tangential electric field, there is a time-average electric surface force density associated with the mechanisms of charge redistribution at the interface. This results in a steady convection which, in the re-entrant geometry, takes the form of the plane Couette flow sketched in figure 2. A method of examining this steady component of electrical surface force density is to measure the shear stress transmitted from the interface to a spring-mounted plate flush with the bottom plate, as shown in figure 2.

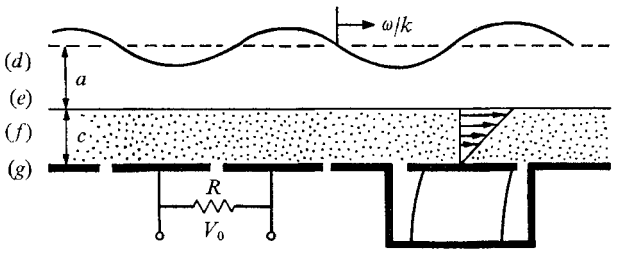

FIGURE 2. Schematic of configuration cross-section for excitation of monolayer by a travelling wave of potential at a predetermined frequency and wavenumber. The electrical response is current induced in bottom electrodes. The time-average shear stress is measured by deflexion of a spring-mounted plate flush with bottom.

Background

The stability of a charge monolayer on an insulating interface has been examined by Melcher & Smith (1969). The tendency of the electric shear stress to redistribute the surface charge so as to make the interface behave as a perfect conductor is brought out by that stability study. As the equilibrium electric field E_0 is increased, instability is incipient at zero frequency, and so studies of incipience uncover only a small part of the picture. Here, we consider the dynamics of the stable interface, and are therefore able to examine the several transfer processes already mentioned.

Previous work on steady convection resulting from interactions between travelling waves of potential and semi-insulating liquids is based on bulk conduction with no uniform component of the charge monolayer (Melcher & Taylor 1969). The pumping mechanism examined here is operative in the limit of a perfectly insulating liquid. Rather than through electrical conduction, the required phase shift between the excitation and periodic component of surface charge is caused by an oscillatory component of the fluid motion itself and the associated convection of space charge.

2. Linear dynamics

Electromechanical coupling

For the present purposes, it is the shearing component T_z of the net surface force density that is most essential to the electrohydrodynamics. In terms of the equilibrium and perturbation surface charge densities, σ_0 and σ_f, and electric field intensity $\mathbf{E} = -\nabla\Phi$,

$$T_z = E_z^e(\sigma_0 + \sigma_f') \cong \sigma_0 \operatorname{Re}(ik\hat{\Phi}^e e^{i(\omega t - kz)}) + \tfrac{1}{2}\operatorname{Re}(ik\hat{\Phi}^e\hat{\sigma}_f^*), \tag{1}$$

where superscripts are used to denote the vertical positions, as indicated in figure 2, $\sigma_0 = \epsilon_0 E_0$ and an asterisk denotes the complex conjugate. The second equality of (1) recognizes that, if the interfacial field and charge are represented by Fourier-type expansions, then there will be a response at the fundamental (ω, k), proportional to the equilibrium charge density and the travelling-wave component of the tangential field, and a steady response independent of z and

proportional to $\hat{E}_z^e \hat{\sigma}_f^*$. Since $\hat{E}_z^e$ and $\hat{\sigma}_f^*$ are both proportional to $\hat{V}_0$, this second time-average part varies like $|\hat{V}_0|^2$ and can be made small relative to the first by making $\hat{V}_0$ small. In this section, attention is given to the linear response which dominates if $\hat{V}_0$ is small, with the steady convection caused by the second term the subject of the next section.

Dynamic equilibrium of the travelling-wave components of shear stress at the interface requires that

$$ik\sigma_0 \hat{\Phi}^e - \hat{S}_z^f = 0, \tag{2}$$

where $\hat{S}_z^f$ is the complex amplitude of the viscous shear stress. Free modes on the interface are essentially of two types: shearing modes, in which the interface remains essentially flat, and modes typified by gravity–capillary waves, in which vertical deflexions of the interface are important. So as to emphasize the former in the following analysis, the interface is taken as suffering only horizontal deflexions. The more complete analysis is straightforward but complex, and is justified when the two types of modes are strongly coupled. This coupling becomes important when the frequency and wavenumber are consistent with those for a free gravity–capillary wave coupled to the equilibrium electric field. Accordingly, the normal-stress equilibrium is ignored in representing the basically shearing dynamics of interest here.

In modelling the conservation of monolayer charge, a mobility b_s is used to represent the mean carrier velocity relative to the neutral fluid, with components defined only in the interfacial plane; surface current density is given by

$$\mathbf{K}_f = \sigma_f b_s \mathbf{E} + \sigma_f \mathbf{v}. \tag{3}$$

Conservation of charge for the interface as a whole requires that

$$(\partial \sigma_f / \partial t) + \nabla_\Sigma . \mathbf{K}_f = \sigma \hat{E}_x^f. \tag{4}$$

Ohmic bulk conduction is represented by the term on the right. In terms of complex amplitudes, (4) (to linear terms) requires that

$$i\omega \hat{\sigma}_f + \sigma_0 b_s k^2 \hat{\Phi}^e - ik\sigma_0 \hat{v}_z^f - \sigma \hat{E}_x^f = 0. \tag{5}$$

Gauss's law specifies the perturbation surface charge density in terms of the normal components of the electric field intensity:

$$\hat{\sigma}_f = \epsilon_0 \hat{E}_x^e - \epsilon \hat{E}_x^f. \tag{6}$$

Bulk dynamics

In the regions above and below the monolayer, the electric potential satisfies Laplace's equation. With α and β used as generic variables representing the upper and lower surfaces of a planar region having thickness Δ, filled by a material of uniform permittivity ϵ and bulk conductivity σ, the 'transfer relations' between the complex amplitudes of surface potentials and normal components of electric field intensity are

$$\begin{bmatrix} \epsilon \hat{E}_x^\alpha \\ \epsilon \hat{E}_x^\beta \end{bmatrix} = \epsilon k \begin{bmatrix} -\coth k\Delta & \dfrac{1}{\sinh k\Delta} \\ -\dfrac{1}{\sinh k\Delta} & \coth k\Delta \end{bmatrix} \begin{bmatrix} \hat{\Phi}^\alpha \\ \hat{\Phi}^\beta \end{bmatrix}. \tag{7}$$

The linear transfer relations for a planar layer of viscous liquid are similarly found from the incompressible Navier–Stokes equations. These take the general form (Zuercher & Melcher 1972)

$$\begin{bmatrix} \hat{S}_x^\alpha \\ \hat{S}_x^\beta \\ \hat{S}_z^\alpha \\ \hat{S}_z^\beta \end{bmatrix} = \frac{1}{F}[P_{ij}(\omega, k)] \begin{bmatrix} \hat{v}_x^\alpha \\ \hat{v}_x^\beta \\ \hat{v}_z^\alpha \\ \hat{v}_z^\beta \end{bmatrix}, \quad \begin{matrix} (8a) \\ (8b) \\ (8c) \\ (8d) \end{matrix}$$

where $\hat{S}_x$ and $\hat{S}_z$ are the normal and tangential components of mechanical stress at the respective boundaries.

Identifying α and β with positions (d) and (e) in (7) so that $\hat{\Phi}^\alpha \to \hat{\Phi}^d = \hat{V}_0$, the fields in the upper region are related by

$$\epsilon_0 \hat{E}_x^e = -(\epsilon_0 k/\sinh ka)\, \hat{V}_0 + \epsilon_0 k \coth ka \hat{\Phi}^e. \tag{9}$$

The potential at the interface is continuous, $\hat{\Phi}^e = \hat{\Phi}^f$, and constrained to be essentially constant on the bottom electrode, $\hat{\Phi}^g = 0$, so (7) can be identified with the layer of liquid, to give

$$\epsilon \hat{E}_x^f = -\epsilon k \coth kc \hat{\Phi}^e, \tag{10}$$

$$\epsilon \hat{E}_x^g = -\epsilon k \hat{\Phi}^e / \sinh kc. \tag{11}$$

The mechanical boundary conditions on the liquid layer are $\hat{v}_x^g = \hat{v}_z^g = 0$ and $\hat{v}_x^f \cong 0$, and hence (8c) gives

$$\hat{S}_z^f = (P_{33}/F)\hat{v}_z^f \equiv \hat{C}\hat{v}_z^f. \tag{12}$$

In the limit of a short viscous skin depth $\delta_v \equiv [2\eta/\omega\rho]^{\frac{1}{2}}$ ($\delta_v \ll c, 2\pi/k$), the complex coefficient $\hat{C}$ becomes simply

$$\hat{C} \to [(1+i)\eta]/\delta_v, \tag{13}$$

while in the opposite limit of creeping flow ($\delta_v \gg c, 2\pi/k$),

$$\hat{C} \to \eta k f(ck); \quad f(ck) \equiv [\sinh 2ck - 2ck]/[\sinh^2 ck - (ck)^2]. \tag{14}$$

Equations (12) and (13) are easily derived from the basic fluid equations. Here, (8) is introduced to emphasize the straightforward procedure for providing the general description.

Frequency response: short viscous skin depth

The self-consistent linear motions are represented in terms of the perturbation surface charge density, interfacial velocity and potential by (2), (5) and (6) with substitution for $\hat{E}_x^e$, $\hat{E}_x^f$ and $\hat{S}_z^f$ from (9), (10) and (12):

$$\begin{bmatrix} 0 & -\hat{C} & ik\sigma_0 \\ j\omega & -ik\sigma_0 & \sigma_0 b_s k^2 + \sigma k \coth kc \\ -1 & 0 & \epsilon_0 k[\coth ka + (c/\epsilon_0)\coth kc] \end{bmatrix} \begin{bmatrix} \hat{\sigma}_f \\ \hat{v}_z^f \\ \hat{\Phi}^e \end{bmatrix} = \begin{bmatrix} 0 \\ 0 \\ \epsilon_0 k \hat{V}_0 / \sinh ka \end{bmatrix}. \tag{15}$$

The electromechanical interfacial response found from (15) is reflected in the current induced in the electrodes below. If each electrode is half a wavelength long and of width d, then the voltage induced across the resistance R has the complex amplitude

$$\hat{v}_0 = (i\omega\epsilon + \sigma)\, dR \hat{E}_x^g \int_0^{\pi/k} e^{-ikz} dz = \frac{i(i\omega\epsilon + \sigma)\, 2dR}{\sinh kc} \hat{\Phi}^e, \tag{16}$$

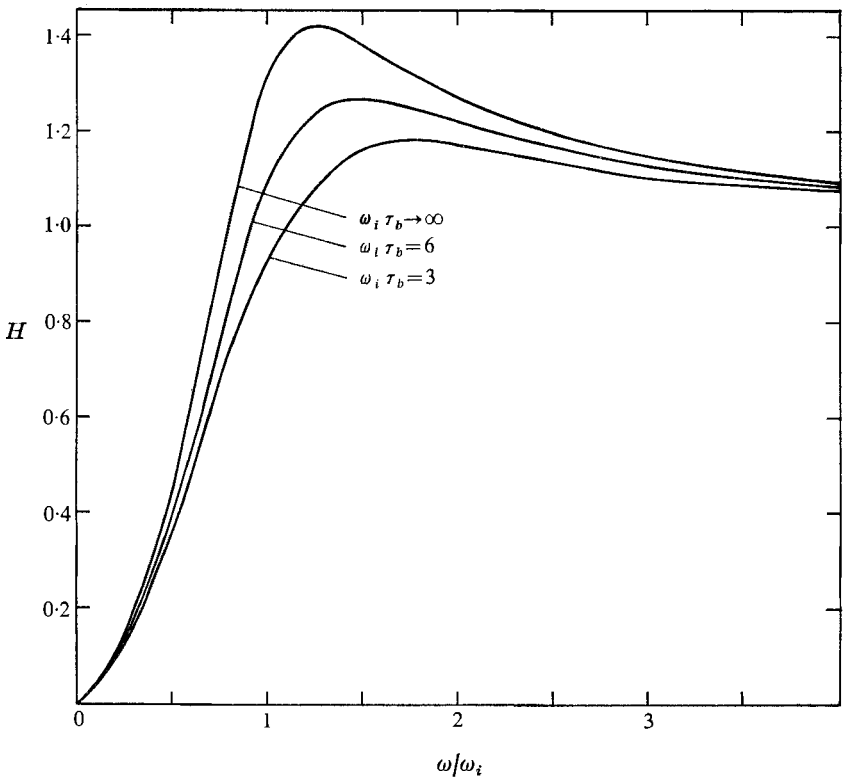

FIGURE 3. The function H characterizing the frequency response, equation (17). Frequency is normalized to the electroviscous frequency ω_i with the effect of surface and bulk conduction on electroviscous resonance illustrated by having the normalized relaxation time τ_b as a parameter.

where (11) is used to write the second expression. In the limit of short viscous skin depth, so that $\hat{C}$ is given by (13), it follows from (15) and (16) that the magnitude of the output voltage normalized to the frequency $f = \omega/2\pi$ is

$$\left|\frac{\hat{v}_0}{f}\right| = \frac{4\pi d R\epsilon\,|\hat{V}_0|\,[1+(\omega\tau_a)^{-2}]^{\frac{1}{2}}}{\sinh ka \sinh kc\,[\coth ka + (\epsilon/\epsilon_0)\coth kc]} H\left(\frac{\omega}{\omega_i}, \omega_i\tau_a\right), \tag{17}$$

where

$$H = \left\{\left[\frac{\omega_i}{\omega}\frac{1}{\omega_i\tau_a} + \left(\frac{\omega_i}{\omega}\right)^{\frac{3}{2}}\frac{1}{\sqrt{2}}\right]^2 + \left[1 - \frac{1}{\sqrt{2}}\left(\frac{\omega_i}{\omega}\right)^{\frac{3}{2}}\right]^2\right\}^{-\frac{1}{2}}.$$

The bulk relaxation time $\tau_a \equiv \epsilon/\sigma$ enters this expression because the sensing electrode is in electrical contact with the liquid, and therefore intercepts a conduction current as well as a charging current. More essential in representing transfer processes occurring at the interface are the electroviscous frequency

$$\omega_i = \left[\frac{k\sigma_0^2}{\epsilon_0(\rho\eta)^{\frac{1}{2}}[\coth ka + (\epsilon/\epsilon_0)\coth kc]}\right]^{\frac{2}{3}} \tag{18}$$

and the combined heterogeneous bulk relaxation and surface relaxation time

$$\tau_b = \frac{\epsilon_0[\coth ka + (\epsilon/\epsilon_0)\coth kc]}{\sigma_0 b_s k + \sigma \coth kc}. \tag{19}$$

For highly insulating fluids having $\omega\tau_a \gg 1$, H characterizes the frequency response. In the short skin depth approximation, and with negligible effect of surface and bulk conduction ($\omega_i\tau_b \to \infty$ in figure 3), there is a resonance in the response peaking at $\omega/\omega_i = 2^{\frac{1}{2}}$. The physical make-up of the associated electroviscous frequency makes it clear that the peak in the response is due to a resonance between charges, which tend to stiffen the interface in the manner of an elastic film, and the mass of the liquid bulk, coupled to the monolayer by the viscous stress. The analogy with purely mechanical film resonances found in studies of monomolecular films on liquid interfaces (Zelazo 1971), is valid provided the wavenumber is fixed. But the electromechanical phenomena comprising the stiffening of the interface here cannot be represented by a surface tension. The energy storage is not uniquely related to the interfacial geometry, but depends as well on the surrounding electrical and mechanical configuration.

As is also illustrated by figure 3, the combined effect of bulk and interfacial conduction represented by τ_b is to attenuate the resonance. In the usual relaxation phenomenon, an $\omega\tau$ of 6 would affect the response by less than 2 %. (See, for example, the bulk relaxation term involving τ_a in the numerator of (17).) But, because of the resonance between inertial and electrical stiffness in the neighbourhood of $\omega = \omega_i$, the response is relatively sensitive to relaxation stemming from either the bulk or the mobility of the interfacial charges.

Frequency response: creeping flow

In the extreme where the inertia of the liquid is negligible, so that (14) is valid, the response function takes the form of (17), but with

$$H = [1 + (\omega\tau_c)^{-2}]^{-\frac{1}{2}}, \tag{20}$$

so that heterogeneous bulk conduction, surface conduction and convection of charge are represented by a single time constant

$$\tau_c \equiv \frac{\epsilon_0[\coth ka + (\epsilon/\epsilon_0)\coth kc]}{\sigma \coth kc + \sigma_0 b_s k + [\sigma_0^2/\eta f(ck)]} \tag{21}$$

and there is no overshoot or resonance in the response. Contributions to the time constants can be distinguished by their dependence on the monolayer charge density σ_0. Note that, if the mobility b_s is inversely proportional to the viscosity (Waldon's rule), surface conduction and convection terms have the same dependence on viscosity.

3. Steady convection

Short viscous skin depth

Steady convection is the result of the uniform component of electric surface force density, the last term in (1). If the viscous skin depth is short compared with the depth c, the total flow can be viewed as an oscillating boundary layer superimposed on steady interfacial streaming, with the latter having an essentially uniform velocity profile over the boundary-layer thickness. In the re-entrant geometry, the flow between this boundary-layer region and the channel bottom

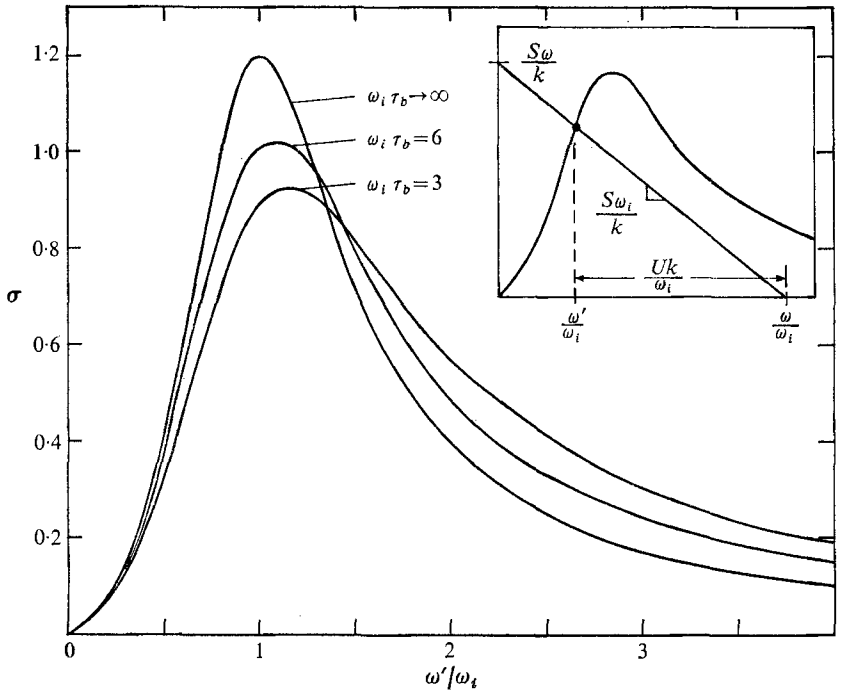

FIGURE 4. Frequency dependence of time-average shearing surface force density showing effect of electrical conduction. In limit $\omega_i\tau_b \to \infty$, all bunching of surface charges is due to electrically induced convection. The frequency ω' is measured in a frame moving with the mean interfacial velocity.

is essentially plane Couette. There is some analogy between this steady response to an oscillatory excitation and streaming associated with oscillatory boundary layers in ordinary fluid mechanics (Batchelor 1970). But here, the streaming velocity U can be large with respect to the amplitude of the fluid oscillations.

Viewed from a frame of reference moving with the mean interfacial velocity U, the oscillatory response is as developed in § 2. In that frame of reference, the frequency is $\omega' = \omega - kU$, and so equations (15) are directly applicable following the substitution $\omega \to \omega'$. Thus, the time-average component of electric surface force density, the last term in (1), is evaluated using (15). To this end, note that, by virtue of (9) and (11), $\frac{1}{2}\operatorname{Re} ik\hat{\Phi}^e \hat{\sigma}_f^* = -\frac{1}{2}\epsilon_0 k^2 \operatorname{Re}(i\hat{V}_0^* \hat{\Phi}^e)/\sinh ka$, so that

$$\langle T_z \rangle = \frac{1}{2} \frac{\epsilon_0 k^2 \hat{V}_0 \hat{V}_0^*}{\sinh^2 ka[\coth ka + (\epsilon/\epsilon_0)\coth kc]} G, \tag{22}$$

where the frequency dependence is characterized by

$$G \equiv \frac{\left[\dfrac{\omega_i}{\omega'}\left(\dfrac{1}{\omega_i\tau_b}\right) + \dfrac{1}{\sqrt{2}}\left(\dfrac{\omega_i}{\omega'}\right)^{\frac{3}{2}}\right]}{\left[1 - \dfrac{1}{\sqrt{2}}\left(\dfrac{\omega_i}{\omega}\right)^{\frac{3}{2}}\right]^2 + \left[\left(\dfrac{\omega_i}{\omega'}\right)\dfrac{1}{\tau_b\omega_i} + \dfrac{1}{\sqrt{2}}\left(\dfrac{\omega_i}{\omega'}\right)^{\frac{3}{2}}\right]^2}. \tag{23}$$

The time-average electric surface force density, like the frequency response of the signal induced on the bottom electrode, is characterized by two clearly

distinguishable time constants. Figure 4 emphasizes the stress induced by the electroviscous coupling by normalizing with the electroviscous frequency the frequency ω' measured in the frame of reference moving with the mean interfacial velocity. In the limit of no conduction, $\tau_b \to \infty$, the maximum stress occurs at $\omega = \omega_i$. Note that, in this limit, the peak magnitude of the time-average surface force is independent of the monolayer charge density. At higher frequencies, the bunching of surface charge is attenuated, while at lower frequencies the surface charge can adjust its distribution in such a way as to cancel the tangential component of electric field. Both effects tend to reduce the surface force density. Surface and bulk conduction tend to broaden the peak. In the extreme where $\omega_i \to 0$, which corresponds to removing the monolayer charge density, the frequency dependence is typical of travelling-wave interactions with media displaying bulk conduction only (Melcher 1966).

Creeping flow

In the creeping-flow limit, the analysis of § 2 is extended to include the steady convection caused by the time-average electric stress using arguments quite different from those for the short viscous skin depth case. In the creeping-flow limit, the fluid mechanics are described by linear equations, and hence the periodic and steady motions can be superimposed. Neither the electrical nor the mechanical volume processes involve time rates of change, which enter only through the conservation of charge boundary condition. Thus, the dynamics viewed from a frame of reference moving with the mean velocity U of the interface are as represented in § 2 with $\omega \to \omega'$ and the understanding that there is a superimposed plane Couette flow.

The time-average electric surface force density found using (14) rather than (13) is given by (22), but with

$$G = \omega' \tau_c / [1 + (\omega' \tau_c)^2]. \tag{24}$$

Here, as in (20), bulk conduction and surface conduction and convection of charge are all lumped into one time constant τ_c, given by (21).

Convection

Equilibrium of time-average electric and viscous stresses at the interface requires that

$$G = \frac{S(\omega - \omega')}{k}; \quad S \equiv \frac{2\eta \sinh^2 ka[\coth ka + (\epsilon/\epsilon_0) \coth kc]}{\epsilon_0 c k^2 |\hat{V}_0|^2}, \tag{25}$$

with $G = G(\omega')$ defined by either (23) or (24) (with $\omega \to \omega'$), as the case may be. This expression is written in such a form that it is convenient to find ω' graphically (see inset to figure 4). The steady velocity is then determined from the relation $U = (\omega - \omega')/k$.

4. Experiment

The steady convection described in § 3 might at first seem the best basis for studying the charge monolayer dynamics. Although simple to provide in ordinary channel flows, unambiguous measurements of velocity in highly insulating liquids stressed by electric fields are difficult to obtain. For example, marker particles suspended in the liquid are inadvertently charged, and as a result, are readily pulled through the liquid by the travelling wave of field. Thus, even though observations have been made of field-induced steady convection of particles floating on the interface, these are not regarded as lending substantive support to the model.

Following a different approach to reflecting the mean convection, a spring-mounted flat plate was suspended flush with the lower electrode. The mean horizontal deflexion was then a measure of the viscous shear stress transmitted to the channel bottom from the time-average electric surface force density at the interface. In principle, such a measurement could be made unambiguous, since there was negligible interference with the field and flow; however, extreme sensitivity was required, and only qualitative observations of the steady component of shear stress can be reported here.

Because electrical measurements could be made relatively sensitive to the surface electromechanics, the frequency response of fields transmitted through the interface was found to be the best basis for experimental study.

The experimental configuration shown in figure 5 was designed so that a single d.c. source of high voltage V_a could be used to provide both the uniform equilibrium field and the travelling wave. The liquid A was contained in a fixed annular channel B having an earthed metal bottom and perspex walls (width 5 cm, mean radius 10 cm). Rod-shaped electrodes, embedded in a perspex disk C, were constrained by the voltage divider to have a spatially periodic potential. Four wavelengths were used, each comprised of 12 electrodes. The potential wave was made to travel by rotating the disk at a frequency subject to mechanical control. The equilibrium electric field and magnitude of the travelling wave were controlled by varying both V_a and the resistance F.

The data shown in figure 6 summarize the frequency response measured using hexane doped with approximately 0·3 % ethyl alcohol. The additive was necessary to make it possible to induce charge at the interface. (Even so, inducing the surface charge without incurring too large a τ_a on the one hand, or on the other hand, too great a sensitivity to minute discharges in the neighbourhood of the interface, was a major source of difficulty.) Runs at three different values of the surface charge density are shown, with the peak amplitude of the travelling wave held fixed at 606 V. (Here, the first Fourier component of the triangular wave was regarded as the actual excitation.) The major source of scatter in the data was the oscilloscope measurement of output voltage; note that the measurements are normalized to the frequency f.

The curves in figure 6 are based on (17) with effects of surface mobility and bulk conduction neglected ($\tau_b \to \infty$). Independent measurement of the bulk conductivity by means of a conductivity cell suggested a bulk relaxation time in excess

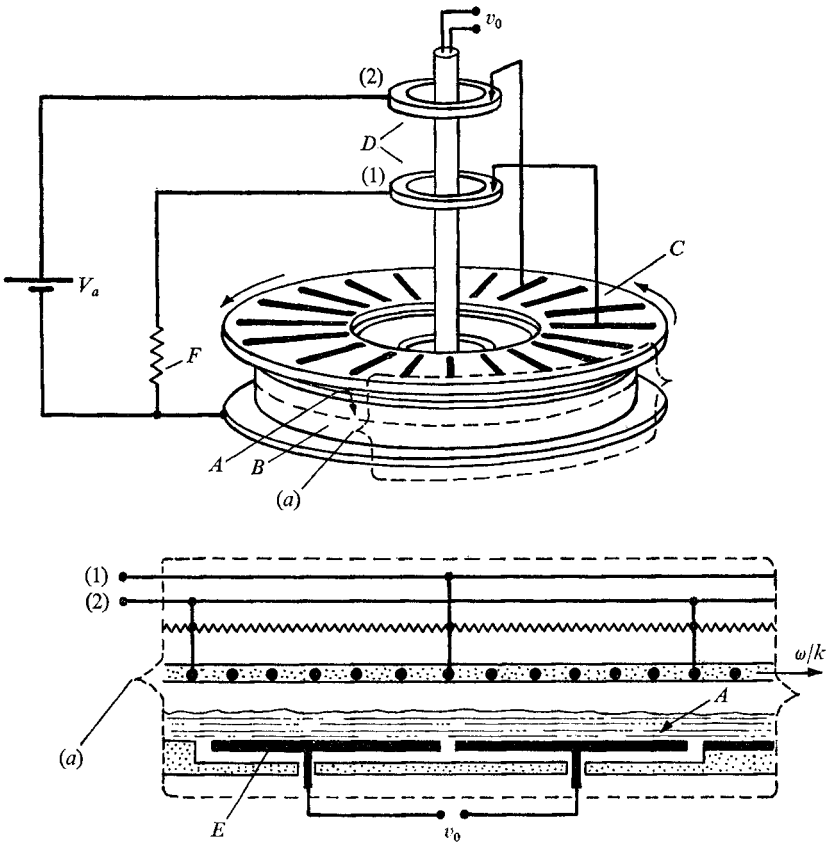

FIGURE 5. Apparatus for measuring frequency response of a field transmitted through a charged interface. The liquid A contained in the annular channel B is stressed by potential on the rotating electrode C having uniform and spatially periodic parts. The liquid slip-rings D and resistance F allow regulation of the equilibrium surface charge and travelling-wave amplitude. The output signal v_0 is induced on the electrodes E.

of 8 s. The discrete electrodes induced somewhat less charge on the interface than would a plane, parallel electrode at the same spacing. The average surface charge was further diminished by the channel walls (which protruded approximately 3 mm above the interface), since these were wetted by the liquid, and hence charged in much the same manner as a conductor. A correction factor of 0·866 was used in determining the value of σ_0 to be used in the theoretical predictions. This factor was based on measurement of the charge induced on a metallic electrode placed at the position of the interface, with the channel walls covered by foil to simulate the effect of the liquid.

The predicted electroviscous resonance and low frequency attenuation is clearly evident from the data of figure 6. Similar results were obtained using carbon tetrachloride, although more difficulty was experienced in controlling the bulk relaxation time. The quantitative agreement between predictions and measurements is quite good for the lowest surface charge density. Although the shift in resonance frequency with increasing charge density is as predicted, there

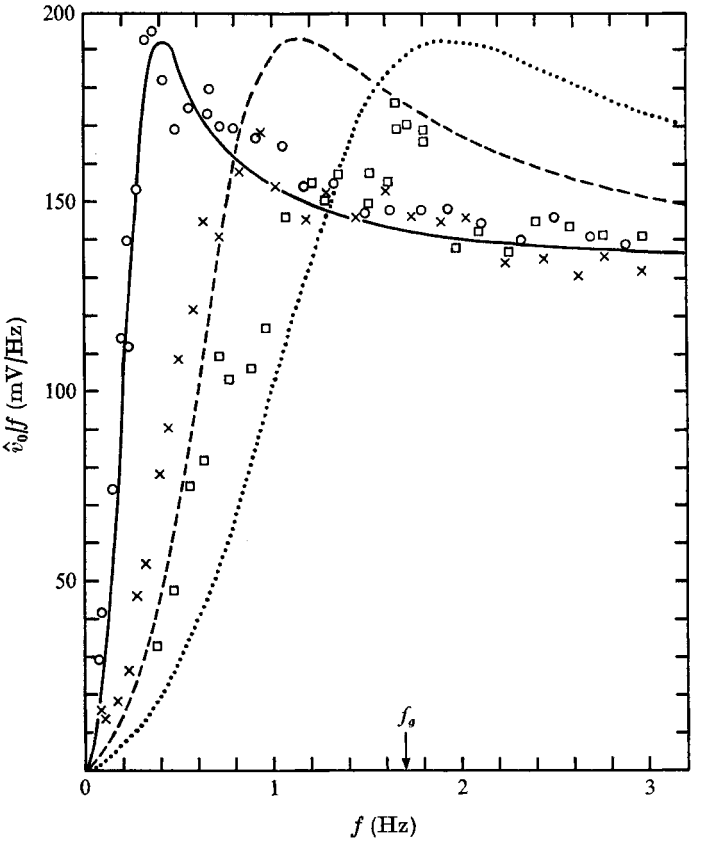

FIGURE 6. Voltage induced on bottom electrode normalized to the frequency $f = \omega/2\pi$ as a function of frequency. Curves, predicted by theory without including damping of resonance which might be attributed to electrical conduction ($\omega_i \tau_b \to \infty$), should be compared with measurements at corresponding surface charge density. The fluid is hexane doped with 0·3% ethyl alcohol, $a = c = 0{\cdot}75$ cm, $\rho = 0{\cdot}69 \times 10^3$ kg/m^3, $\eta = 0{\cdot}374 \times 10^{-3}$ N/m^2, $\epsilon/\epsilon_0 = 1{\cdot}89$. ○—○, $\sigma_0 = 1{\cdot}8 \times 10^{-6} Q$ m^{-2}; × -- ×, $\sigma_0 = 3{\cdot}9 \times 10^{-6} Q$ m^{-2}; □ ··· □, $\sigma_0 = 6{\cdot}0 \times 10^{-6} Q$ m^{-2}.

is clearly a decrease in the 'Q' of the response with increasing σ_0 that is not predicted by the theory with $\tau_b \to \infty$.

It might be conjectured that the damping of the resonance is a result of an increased role for the surface mobility. According to (19), τ_b is decreased by increasing σ_0. But, as is evident from figure 3, the damping is determined by $\omega_i \tau_b$, and that quantity is proportional to $\sigma_0^{\frac{1}{3}}$. So, if the surface mobility is constant, the 'Q' of the response should increase slightly, rather than decrease, with increasing surface charge density.

5. Concluding remarks

There are several plausible reasons that can be put forward for the attenuation of the resonance with increasing surface charge density. First, the coupling to the gravity–capillary type of surface-wave (transverse) modes is not included in the

theoretical response. Although somewhat revised by the electric field, the frequency of a gravity wave with the same wavelength as the excitation closely approximates that of the field-coupled wave system. This is the frequency f_g denoted in figure 6. In the neighbourhood of this frequency, a large vertical deflexion was excited which travelled in phase with the excitation wave. The output signal, typically, was complicated by 'beats' in this range, tending to introduce additional scatter in the measured signal. This accounts for scatter in the data obtained at high charge density in the neighbourhood of f_g. Of course, the response should be purely sinusoidal, regardless of whether or not the coupling to the transverse modes is significant, but because of the relatively high 'Q' of the transverse mode, the control of physical dimensions and the periodicity of the travelling wave was more critical in this range. To examine the details in the immediate range of f_g would require greater control of physical parameters than was available in the experiment; in any case, it is expected that the anti-resonance typical of coupling to the gravity mode (Zuercher & Melcher 1972; Zelazo 1971) would tend only to attenuate the signal in the range of perhaps 0·2 Hz around f_g.

A second possibility is that, with increasing field intensity, further loss mechanisms come into play which have a damping effect similar to that of conduction in the liquid – for example, ionization of the air above the interface or instability of the interface at wavelengths far shorter than those being excited. In fact, there is visual evidence that a fine-scale mixing occurs on the interface at high field strengths.

Probably the most fundamental of the possibilities is that the lumped surface parameter model (surface charge density and surface mobility) does not give a complete picture of the dynamics of a diffuse monolayer of charge. This last possibility can be investigated by using the same 'imposed (ω, k)' approach used here, but describing the self-consistent motions with the structure of the layer included in the analysis.

This work was carried out while the author was on Sabbatical leave from the Massachusetts Institute of Technology as an Overseas Fellow at Churchill College, supported by the Winston Churchill Foundation of the United States, and a Guggenheim Fellowship; he was a guest of the Department of Applied Mathematics and Theoretical Physics at Cambridge University. With the constant encouragement and many suggestions of G.I. Taylor, the experimental work was performed in his laboratory at the Cavendish. The rotating electrode structure used in these experiments was mounted on the same apparatus as used by G.I. Taylor for experiments on the shear flow in porous material (Taylor 1971). Invaluable technical assistance came from Mr George Garner and members of Dr Townsend's Fluid Mechanics Section.

REFERENCES

BATCHELOR, G. K. 1970 *An Introduction to Fluid Mechanics*, pp. 353–364. Cambridge University Press.

DELAHAY, P. 1965 *Double Layer and Electrode Kinetics*, chap. 3. Interscience.

MELCHER, J. R. 1966 Traveling-wave induced electroconvection. *Phys. Fluids*, **9**, 1548–1555.

MELCHER, J. R. & SMITH, C. V. 1969 Electrohydrodynamic charge relaxation and interfacial perpendicular-field instability. *Phys. Fluids*, **12**, 778–790.

MELCHER, J. R. & TAYLOR, G. I. 1969 Electrohydrodynamics: a review of the role of interfacial shear stresses. *Ann. Rev. Fluid Mech.* **1**, 111–146.

TAYLOR, G. I. 1971 *J. Fluid Mech.* **49**, 319.

ZELAZO, R. E. 1971 Dynamic interactions of monomolecular films with imposed electric fields. Ph.D. thesis, Department of Electrical Engineering, Massachusetts Institute of Technology.

ZUERCHER, J. C. & MELCHER, J. R. 1972 Double-layer transduction with imposed temporal and spatial periodicity. Submitted for publication.